IVYSPRING INTERNATIONAL PUBLISHER

Theranostics

2019; 9(8): 2395-2410. doi: 10.7150/thno.29422

Research Paper

Donation of mitochondria by iPSC-derived mesenchymal stem cells protects retinal ganglion cells against mitochondrial complex I defect-induced degeneration

Dan Jiang[1,2,3], Guoyin Xiong[1], Hong Feng[4], Zhao Zhang[3,4], Peikai Chen[5], Bin Yan[5], Ling Chen[4], Kesavamoorthy Gandhervin[1], Chuiyan Ma[4], Cheng Li[4], Shuo Han[4], Yuelin Zhang[4], Can Liao[3], Tin-Lap Lee[6], Hung-Fat Tse[4], Qing-Ling Fu[7]✉, Kin Chiu[1,8,9]✉, Qizhou Lian[4,1,3,10]✉

1. Department of Ophthalmology, The University of Hong Kong, Hong Kong SAR, P.R. China
2. Lab for Stem Cell & Retinal Regeneration, Institute of Stem Cell Research, The Eye Hospital, Wenzhou Medical University, Wenzhou, P.R. China
3. Guangzhou Women and Children's Medical Center, Guangzhou Medical University, Guangzhou, P.R. China
4. Department of Medicine, The University of Hong Kong, Hong Kong SAR, P.R. China
5. School of Biomedical Sciences, Li Ka Shing Faculty of Medicine, The University of Hong Kong, Hong Kong SAR, P.R. China
6. School of Biomedical Sciences, Faculty of Medicine, the Chinese University of Hong Kong, Hong Kong SAR, P.R. China
7. Otorhinolaryngology Hospital, The First Affiliated Hospital, Sun Yat-sen University, Guangzhou, P.R. China
8. The State Key Laboratory of Brain and Cognitive Sciences, The University of Hong Kong, Hong Kong SAR, P.R. China
9. GHM Institute of CNS Regeneration, Jinan University, Guangzhou, P.R. China
10. The State Key Laboratory of Pharmaceutical Biotechnology, The University of Hong Kong, Hong Kong SAR, P.R. China.

✉ Corresponding authors: Dr. Qizhou Lian, E-mail: qzlian@hku.hk; Dr. Kin Chiu, E-mail: datwai@hku.hk; Dr.Qingling Fu, E-mail: fuqingl@mail.sysu.edu.cn

Received: 2018.08.23; Accepted: 2019.03.05; Published: 2019.04.13

Abstract

Rationale: Retinal ganglion cell (RGC) degeneration is extremely hard to repair or regenerate and is often coupled with mitochondrial dysfunction. Mesenchymal stem cells (MSCs)-based treatment has been demonstrated beneficial for RGC against degeneration. However, underlying mechanisms of MSC-provided RGC protection are largely unknown other than neuroprotective paracrine actions. In this study, we sought to investigate whether mitochondrial donation from induced pluripotent stem cell-derived MSC (iPSC-MSCs) could preserve RGC survival and restore retinal function.

Methods: iPSC-MSCs were injected into the vitreous cavity of one eye in NADH dehydrogenase (ubiquinone) Fe-S protein 4 (*Ndufs4*) knockout (KO) and wild type mice. Phosphate buffer saline (PBS) or rotenone treated iPSC-MSCs were injected as control groups. Retinal function was detected by flash electroretinogram (ERG). Whole-mount immunofluorescence (IF), morphometric analysis, confocal microscopy imaging, polymerase chain reaction (PCR) of the retinas were conducted to investigate mitochondrial transfer from human iPSC-MSCs to mouse retina. Quantitative mouse cytokine arrays were carried out to measure retinal inflammatory response under difference treatments.

Results: RGC survival in the iPSC-MSC injected retina of *Ndufs4* KO mice was significantly increased with improved retinal function. GFP labelled human mitochondria from iPSC-MSC were detected in the RGCs in the retina of *Ndufs4* KO mice starting from 96 hours post injection. PCR result showed only human mitochondrial DNA without human nuclear DNA could be detected in the mouse retinas after iPSC-MSC treatment in *Ndufs4* KO mice eye. Quantitative cytokine array analysis showed pro-inflammatory cytokines was also downregulated by this iPSC-MSC treatment.

Conclusion: Intravitreal transplanted iPSC-MSCs can effectively donate functional mitochondria to RGCs and protect against mitochondrial damage-induced RGC loss.

Key words: mitochondrial defect, induced pluripotent stem cell derived-mesenchymal stem cell, mitochondrial transfer, retinal ganglion cell

Introduction

Exogenous administration of mesenchymal stem cells (MSC) protects retina from degenerative diseases, including glaucoma and Leber's hereditary optic neuropathy (LHON) [1-4], suggesting that MSCs might be neuroprotective to the retinal ganglion cells (RGC) in this context. Several on-going clinical trials indicate the feasibility and safety of using MSCs for the treatment of neuromyelitis optical disorders (www.clinicaltrials.gov, NCT01920867; NCT02249676) and age-related macular degeneration (AMD) (NCT02016508). Current understanding on MSCs mediated preservation on retinal function is either through direct replacement of damaged neuron [5-9], or indirect neuroprotective factors secretion to support stressed retinal neurons [2, 10-12]. Unfortunately, neither of these hypotheses could fully elucidate the mechanisms of MSC-induced retinal protection [13].

RGCs are responsible for propagating signals derived from visual stimuli in the photoreceptor cells in the retina, through their long axons, to the lateral geniculate body/superior colliculus in the brain [14, 15]. Due to the natural complexity of RGCs in neuronal development, axon guidance, and complex synaptic connections, it has been difficult to achieve neuroprotection and neural regeneration once damaged, as in glaucoma or LHON [16-20]. Moreover, there is an inner limiting membrane (ILM) lining the boundary between the retina and the vitreous body which formed by astrocytes and the end feet of Müller cells. It prevents free access of intra vitreous drug/cells to the retina [21]. Whether the intravitreal administration of MSCs could protect RGCs from mitochondrial deficiency-related stress or stress-induced neurodegeneration requires further investigation.

Increasing evidence indicates that MSCs can transfer their mitochondria to pheochromocytoma PC12 cells, lung airway cells, cardiomyocytes, corneal cells, astrocytes and neural cells, and improve mitochondrial bioenergetics [22-28]. It is speculated that MSCs transfer mitochondria through tunneling nanotubes (TNT) or microvesicles into the recipient cells. Our previous study demonstrated both human adult bone marrow-derived MSC (BM-MSC) and induced pluripotent stem cell-derived MSC (iPSC-MSC) efficiently donated functional mitochondria to affected bronchoalveolar epithelial cells to rescue cigarette smoke-induced chronic obstructive pulmonary disease (COPD) [29]. Of note, the efficiency of functional mitochondria donated from iPSC-MSCs was much higher than adult BM-MSC to rejuvenate heart and lung injuries [29-31]. The difference in the mitochondria donation is proposed link to the higher expression of intrinsic Rho GTPase 1, mitochondrial motility regulator Miro1 or enhanced response to tumor necrosis factor alpha (TNF-α)-induced TNT formation in the iPSC-MSC.

Mitochondrial transfer from the MSC to neuron was previously demonstrated through cell-to-cell contact in both cell culture system and in live animals [27, 28]. The existence of TNT between MSC and neuronal cell might be a very important contributing factor for neuroprotective effects through mitochondria transfer. However, ILM exist as the challenge for mitochondria transfer through TNT to RGC when the iPSC-MSC is transplanted in the vitreous cavity. In the current study, we sought to examine whether iPSC-MSCs can donate mitochondria to retinal cells and protect RGC against mitochondrial deficit-induced retinal degeneration.

To investigate this hypothesis, we used a mitochondrial complex I (NADH: ubiquinone oxidoreductase) deficiency mouse model that carries mutation in NADH dehydrogenase [ubiquinone] iron-sulfur protein 4 (*Ndufs4*) gene [32]. *Ndufs4* KO mice originally developed as a model of Leigh's disease, an encephalomyelopathic disease resulting from complex I defect in the brain that results in infantile death. Mitochondrial complex I deficiency in the KO mice retina induced innate immune and inflammatory markers associated with loss of RGC function and death [33]. Here we reported the effect of intravitreal injected human iPSC-MSCs to rescue mouse RGCs through mitochondria transfer, but not direct stem cell replacement. Furthermore, our cytokine array analysis demonstrated the alternation in pro-inflammatory cytokines after mitochondrial transfer. Our study provided the evidence that the functional mitochondria from intravitreously injected iPSC-MSCs migrated across the ILM and protected RGCs from the mitochondria deficiency-induced degeneration.

Methods

Ndufs4 knockout mouse model

All laboratory procedures on mice were approved by the committee on the Use of Live Animals in Teaching and Research (CULATR) of The University of Hong Kong. Mice were housed in a minimal disease area (MDA) under controlled environmental conditions on a 12 hours light-dark cycle with *ad libitum* access to food and water at room temperature (about 22°C). C57BL/6 mice were crossed with *Ndufs4*+/− mice for colony maintenance. To acquire *Ndufs4*−/− (KO) and *Ndufs4*+/+ (WT) mice, heterozygous (*Ndufs4*+/−) male mice were mated with female mice.

Electroretinography for retinal function detection

To evaluate the visual function of WT and KO *Ndufs4* mice, photopic flash electroretinography (ERG) was performed with Espion ERG Diagnosys machine (Diagnosys, USA). To demonstrate the effect of iPSC-MSC treatment, ERG was performed at 1 and 4 weeks after injection. Before ERG test, mice were anesthetized by i.p. injection of ketamine (100 mg/kg) and xylazine (20 mg/kg), pupils were dilated using with 1% Mydriacyl (Alcon, US). Both eyes were anesthetized topically with 0.5% proparacaine (Alcon, US), ring shaped gold recording electrodes were placed on the cornea of both eyes. A pair of reference needle electrodes made of stainless steel were placed subcutaneously behind the ears and a ground electrode was placed subcutaneously by the tail. After 10 min green light adaption, eyes of the tested mouse were exposed to a series of light flashes in increasing intensities of 11.38 cd.s/m^2, 16.60 cd.s/m^2 and 22.76 cd.s/m^2 with a green background, to record the light response of the retinas. Mice's body temperature was maintained at 37°C by a heating pad during the whole procedure. Results were analyzed for a-wave, b-wave, and PhNR by ERG View v4.380R software.

Evaluation of RGC survival in whole mount retina

At 3 different time points (96 hours, 1 week, and 4 weeks), eyes were enucleated and fixed in 4% paraformaldehyde in PBS for 30 mins at 4 °C followed by a cornea puncture and extra 30 mins fixation. Then the anterior segment was removed and the retina was detached carefully from the underlying RPE and sclera. To evaluate RGC survival, RGCs were labeled with brain-specific homeobox/POU domain protein 3A (Brn3a, SC-31984, Santa Cruz Biotechnology, TX, USA) for the nucleus or tubulin beta 3 (TUBB3, 657402, Biolegend, CA, USA) for the cytoskeleton were counted in whole mount retina. After soaking with 5% BSA and 0.5% Triton-X-100 in PBS for 1 hr, the retinas were incubated with primary antibody (1:500) at 4 °C overnight followed by secondary antibody (Alexa Fluor 488, A-21467; Alexa Fluor 568, A-11019; Invitrogen, USA, 1:1000) at room temperature for 2 hours. After 3~6 times of washing with PBST, retinal tissue was flatted with retinal ganglion cell layer facing up on a glass slide and mounted. RGC number was counted as Brn3a positive labeled RGCs on flat mounted retinas (Figure 1B) from superior, inferior, nasal and temporal retinal region. Four individual fluorescent images from aforementioned four regions and sixteen regions per retina were taken using the fluorescent microscope (Leica laser microscope 700/800, Germany). Each region included four areas from central to peripheral retina, shown as central (C-R), near-peripheral (N-P), mid-peripheral (M-P) and far-peripheral (F-P) retina in Figure 1B. RGC number counted on the photos and RGC density at per mm square unit was averaged from the sixteen regions per eye.

Morphometric analysis of the vertical retinal sections

Eyes from KO and WT mice at 3, 4 and 7 weeks old were collected and processed for paraffin vertical sections, followed by standardized Hematoxylin and Eosin (H&E) staining protocol. H&E retinal images were taken from 2 retinal areas: Central retina (C) and peripheral retina (P). The thickness of inner nuclear layer (INL), inner plexiform layer (IPL) were measured by ImageJ software.

Cell culture and mitochondrial labeling

Human iPSC-MSCs [34] as the mitochondria donor cells were prepared and cultured in Dulbecco modified Eagle's medium (DMEM; Gibco, Invitrogen, USA) plus 15% fetal bovine serum (FBS), 2 ng/ml EGF and 2 ng/ml FGF [34]. To evaluate the effectiveness of mitochondrial transfer, the iPSC-MSCs were transfected with Lentiviral-Mitochondrial-Green Fluorescence Protein (LV-Mito-GFP) [26, 29], following the published protocol for a 3rd generation lentiviral packaging system designed by Dull T et al. [35]. This system contained 3 plasmids in total, including two packaging plasmids and one envelope plasmid. A transfer plasmid, mito-GFP (mitochondria COX8 Tag, CYTO102-PA-1-SBI), was bought from SBI System Bioscience. iPSC-MSCs pretreated with mitochondrial complex I inhibitor rotenone (R) (50 nM for 2 hours) was named as iPSC-MSCs(R) and served as the mitochondria viability control group [26].

Primary cultures of RGCs were prepared from the isolated retina ($n \geq 8$/preparation) of 2 to 4 days old mice [36]. CD90.1 MicroBeads (Miltenyi Biotec, Germany) were used to isolate RGCs from retinal cell suspension. For the co-culture experiment with iPSC-MSCs, RGCs as the recipient cells were labeled with CellTrace Violet (Excitation: 405, C34557, Invitrogen, USA).

Intravitreal injection

To evaluate the effect of mitochondrial intercellular transfer from iPSC-MSCs to the *Ndufs4-/-* retinas, iPSC-MSC treatment was performed via intravitreal injection. iPSC-MSCs, PBS, or iPSC-MSCs(R) were respectively injected into the vitreous body of *Ndufs4-/-* mice at 3 weeks postnatal. Cell suspension containing 1×10^4 iPSC-MSCs/ iPSC-MSCs(R) in 0.5 µL PBS was slowly injected into

the vitreous cavity of the mice under anesthesia (Ketamine (100 mg/kg) and xylazine (20 mg/kg), i.p. injection). The same volume of PBS was injected as the control group. At 96 hours, 1 week, and 4 weeks after injection, mice were sacrificed for examination. Eyes with either cataract or vitreous hemorrhage after the injection were excluded from the study. Experimental procedure was displayed in Figure S1.

Assessment of mitochondrial transfer and Müller cell activation

Mitochondrial transfer was detected via immunofluorescence on flat mounted retina. To observe mitochondrial transfer to the retina following iPSC-MSC injection, TUBB3 was used to label neuronal cytoskeleton and Brn-3a was used to stain the nucleus of RGCs. Antibody against GFP (anti-GFP; RA5-22688, Invitrogen, USA), or against human mitochondria (anti-hMito; ab92824, Abcam, USA) were used to label human mitochondria originated from iPSC-MSCs. Anti-human nuclear antigen (HNA; Millipore, USA) was used to identify human cells. Retinal samples were examined using a laser scanning confocal microscope LSM700 or a time-lapse video recorder. To identify the precise location of the mitochondria in the mouse retina, z-stack scanning strategy, and orthogonal section of the retina were carried out for further image analysis. Evaluation of the average immunoreactivity of GFP signal from the retinal ganglion cell layer (GCL) was compared among different time points of post iPSC-MSC treatment.

To evaluate Müller cell activation following iPSC-MSC therapy, immunohistochemistry of glial fibrillary acidic protein (GFAP; G3893, Sigma, USA) on the retinal sections was performed.

Polymerase chain reaction (PCR)

To avoid contamination of the iPSC-MSC attached to the ILM, vitreous body was carefully removed with forceps under dissection microscope. Total DNA of the retina was extracted using a DNA kit (Qiagen, USA). 1 μg of total DNA was used as a template for PCR. PCR cycles were as follows: 94 °C for 5 mins, 35 cycles at 94 °C for 20 seconds, 57 °C for 30 seconds, 72 °C for 40 seconds, and a final extension at 72 °C for 5 mins. The amplified products were analyzed by electrophoresis in 1.0% agarose gel containing ethidium bromide. The primers used in this study were human specific mitochondria DNA (mtDNA), Forward 5'-ACCACCCAAGTATTGACT CACC-3', Reverse 5'-GGGGGTTTTGATGTGGATT GG-3'; murine specific mtDNA, Forward 5'-AGGCATGAAAGGACAGCACA-3', Reverse 5'-TTGGGGTTTGGCATTAAGAGGA-3'; human specific nuclear DNA (nDNA), Forward 5'-GCATCGTGCTGCCTTGATTT-3' Reverse 5'-CCGT AAGAGGCCAGCACATT-3'; murine specific nDNA, Forward 5'-GAATTCAGATTTGTGCATACACAGTG ACT-3' and Reverse 5'-AACATTTTTCGGGGAATAA AAGTTGAGT-3'.

Quantified inflammatory cytokines array of retina

Retinas were isolated from mice and snap frozen for analysis of inflammatory cytokines. The concentration of 40 cytokines was determined using the Quantibody Mouse Inflammation Array Kit according to the manufacturer's instructions (RayBiotech, Inc., Norcross, USA). The array was designed to quantitatively detect 40 inflammatory cytokines: BLC (CXCL13), CD30 Ligand (TNFSF8), Eotaxin-1 (CCL11), Eotaxin-2 (MPIF-2/CCL24), Fas Ligand (TNFSF6), GCSF, GM-CSF, I-309 (TCA-3/CCL1), ICAM-1 (CD54), IFN-gamma, IL-1 alpha (IL-1 F1), IL-1 beta (IL-1 F2), IL-10, IL-12 p70, IL-13, IL-15, IL-17A, IL-2, IL-21, IL-3, IL-4, IL-5, IL-6, IL-7, KC (CXCL1), Leptin, LIX, MCP-1 (CCL2), MCP-5, M-CSF, MIG (CXCL9), MIP-1 alpha (CCL3), MIP-1 gamma, Platelet Factor 4 (CXCL4), RANTES (CCL5), TARC (CCL17), TIMP-1, TNF alpha, TNF RI (TNFRSF1A) and TNF RII (TNFRSF1B). Signals (green fluorescence, Cy3 channel, 555 nm excitation, and 565 nm emission) were captured using a GenePix 4000B laser scanner (Bio-Rad Laboratories, Hercules, USA) and extraction performed with GenePix Pro 6.0 microarray analysis software. Quantitative data analysis was performed using RayBiotech mouse Inflammation Array 1 software (QAM-INF-1_Q-Analyzer). Sample concentrations (pg/ml) were determined from mean fluorescence intensities (median values) compared with five-parameter linear regression standard curves generated from standards provided by the manufacturer.

Statistical analysis

Statistical analysis was performed using Prism 5.04 Software (GraphPad Software for Windows, San Diego, USA), and results are reported as mean ± S.D. Comparisons between more than two groups were analyzed by one-way ANOVA test. Comparisons between two groups were performed using Student's t-test, p-value <0.05 was considered statistically significant.

Results

Ndufs4 deficient induced retinal degeneration in mice

Due to the mitochondrial deficiency, the lifespan of *Ndufs4* KO mice is about 9 weeks. To investigate the temporal changes of the mice retina and find the

optimal therapeutic window, *Ndufs4* KO mice aged from week 3 to 7 were analyzed. Retinal function test showed significant reduction in b-wave and PhNR amplitudes started from 4 weeks postnatal in KO mice compared to WT (*Ndufs4*+/+) mice (Figure 1A, *p<0.05). RGC number was counted as Brn3a positive labeled RGCs on flat mounted retinas (Figure 1B). Compared to WT retinas, the density of RGC in KO mice significantly decreased starting at week 6. At week 7, significant reduction in entire retinal inner plexiform layer (IPL) thickness, and peripheral retinal inner nuclear layer (INL) thickness were detected in H&E stained retinal sections (Figure 1C).

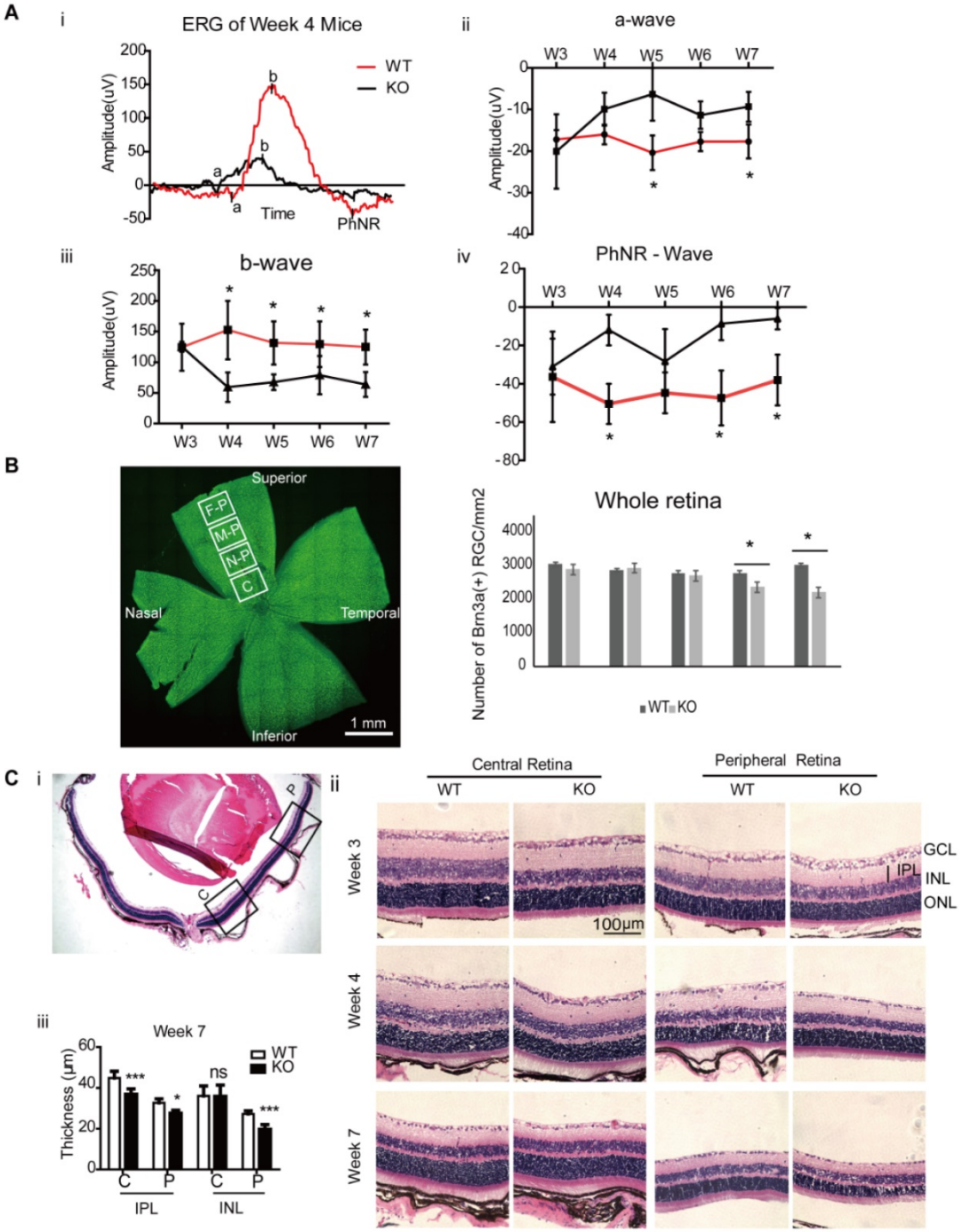

Figure 1. Retinal Changes in *Ndufs4* deficient mice. A. Retinal function analysis by electroretinogram (ERG) with flash intensity at 16.60 scd/m². A representative ERG wave in WT and KO mice at 4 weeks of age (i), and the amplitude changes in mice ERG from 3 weeks to 7 weeks at a-wave (ii), b-wave (iii) and PhNR-wave (iv). Compared to WT (*Ndufs4*+/+) mice, significant amplitudes reduction in b-wave and PhNR started from age 4 weeks in KO mice (*p<0.05, n=10). **B.** The left panel showed whole mount retina with the four analyzed regions: central (C), near-peripheral (N-P), mid-peripheral (M-P) and far-peripheral (F-P) retina. Number of Brn3a positive RGCs in whole mounted retina from *Ndufs4* KO and WT mice between 3 weeks to 7 weeks old were counted in the right panel. (n=5 eyes/group). **C.** Hematoxylin and Eosin (H&E) stained retinal sections of 3, 4, and 7 weeks old *Ndufs4* KO and WT mice. (i) Selected regions of the central and peripheral retina were labeled to study the structural changes. (ii) H&E images of central and peripheral retina. (iii) Thickness of inner nuclear layer (INL), inner plexiform layer (IPL) were measured (n=5). Data are represented as mean values ± SD. *p<0.05, **p<0.01, ***p<0.001, ns, not significant (Student's t-test).

Similar to the retinal changes of LHON patient, current result confirmed that mitochondrial complex I dysfunction in the retina induced retinal function defects with progressive loss of RGC in the *Ndufs4* KO mice. At week 3, there was no significant functional and pathological difference between KO and WT *Ndufs4* mice. The retinal function reduction started at age of week 4, followed by significant RGC loss at week 6 and then marked thinning of IPL and INL indicated the involvement of other inner retinal neurons at week 7. Collectively, these results indicate treatment or mitochondrial transfer before week 4 in *Ndufs4* KO mice might prevent the progressive loss of retinal function and RGCs. In the following part, we performed intravitreal injection of iPSC-MSC at week 3 and examined the mouse retinas at 96 hours, 1 week and 4 weeks post injection (Figure S1).

Administration of iPSC-MSCs prevented retinal function decline in *Ndufs4* KO mouse

Effectiveness of iPSC-MSC on retinal protection was first evaluated by retinal function tests. Intravitreal injection were carried out at 3 weeks of age of mice and retinal function test ERG was performed at 1 week and 4 weeks after the injection right before eye sample collection. Compared with age-matched WT mice receiving PBS injection (WT-PBS) at 1-week post-surgery, Ndufs4 mice (KO-PBS) showed significant reduction in amplitude of PhNR (from -26.87 μV to -5.98 μV), which implicated the malfunction of the RGC in KO mice at age of 4 weeks with PBS injection (Figure 2A iii, ***p<0.001). Intravitreal injection of iPSC-MSC effectively preserved the PhNR value at -27.96 μV in KO+iPSC-MSC group (Figure 2A iii, ***p<0.001 vs KO-PBS, vs KO+ iPSC-MSC (R) group), but Rotenone pretreatment on iPSC-MSC (-3.50 μV) showed no protective effect on RGC function and was at similar level in KO-PBS group. There was no significant difference in b-wave among all four groups (Figure 2Aii) while significant reduction was detected in a-wave when compared KO+iPSC-MSC(R) (-6.39 μV) with KO+iPSC-MSC (-10.56 μV) (Figure 2Ai, **p<0.01).

At the 4 weeks after injection, there was amplitude decrease in a, b, and PhNR in the KO+PBS mice compared to those of 1 week after injection. At 4 weeks after injection, there was no significant difference in the amplitude of a wave (Figure 2Bi). Significant reduction of the amplitude in b wave in KO-PBS (45.08 μV) compared to WT-PBS (94.20 μV) was detected (Figure 2Bii, *p<0.05), indicating the malfunction of inner retina such as bipolar cell and Müller cell function. A single intravitreal injection of iPSC-MSC at week 3 could not reverse the change at week 7 for the b wave. While the PhNR amplitude preservation was observed after 4 weeks treatment in the KO+iPSC-MSC group (-18.08 μV) compared to the KO+PBS group (-10.98 μV). Taken together, a single injection of 1×10^4 healthy iPSC-MSC at the vitreous body enhanced RGCs function significantly till 4 weeks after treatment.

Prevention of RGC loss with iPSC-MSCs treatment in *Ndufs4* KO mice

To determine whether iPSC-MSC administration prevents RGC loss in the *Ndufs4* mouse retina, we performed intravitreal injection of iPSC-MSCs into 3 week old *Ndufs4* KO mice. Age and sex matched KO mice were divided into three groups randomly and subjected to one of the following: iPSC-MSC treatment (KO+iPSC-MSC), vehicle treatment (KO+PBS), iPSC-MSC pre-treated with rotenone to induce dysfunctional mitochondria (KO+iPSC-MSC(R)). WT littermate mice with vehicle administration served as controls (WT+PBS). After 1 week of treatment (at 4 weeks postnatal), the density of RGCs did not differ significantly among WT+PBS, KO+PBS and KO+iPSC-MSC group. Surprisingly, there was marked loss of the RGCs in the KO+iPSC-MSC(R) group compared with the other three groups (Figure 2C, p<0.05). These results provided an important warning that transplantation iPSC-MSC with mitochondrial dysfunction not only did not have the capacity for RGC protection but also harmful to RGC homeostasis, leading to RGC loss. At 4 weeks after intravitreal injection (mice at 7 weeks of age), density of RGC in vehicle treated retina (PBS control group) in the *Ndufs4* KO mice was significantly reduced compared with WT mice (Figure 2C, ***p<0.001). iPSC-MSC administration significantly prevented RGC loss compared with vehicle treatment in *Ndufs4* KO mice (Figure 2C, *p<0.05). Once the mitochondrial function was inhibited by rotenone in the iPSC-MSC, the density of the RGC in the iPSC-MSC(R) treated group was significantly decreased compared to that of iPSC-MSC treated group (Figure 2C, *p<0.05) and vehicle treated group (Figure 2C). These results confirmed the RGC survival was tightly associated with functional mitochondria of iPSC-MSC in the stressed retinal environment.

iPSC-MSCs transferred mitochondria to neurons in retinal ganglion cell layer

To detect whether intravitreally injected iPSC-MSCs could transfer human mitochondria to mouse retinal cells, mitochondria of iPSC-MSCs were genetically labeled with LV mito-GFP prior to intravitreal injection [29]. Since we only conducted a

single intravitreal injection of iPSC-MSC at age week 3 in the KO mice. The mito-GFP signal must be enhanced by immunostaining for quantitative morphometric analysis among different time points. Anti-GFP primary antibody was used (Figure 3A i, lane 2) and then the long-term transfer efficiency of mitochondria to the cells in the GCL were analyzed. No GFP signal in the GCL from the PBS control group (Figure 3A i) confirmed the specificity of the immunostaining. Mean fluorescence intensity (in arbitrary unit) of GFP positive mitochondria increased as early as 96 hours and maintained up to 4 weeks with the highest transfer rate at 1 week after injection (*P<0.05, Figure 3A ii).

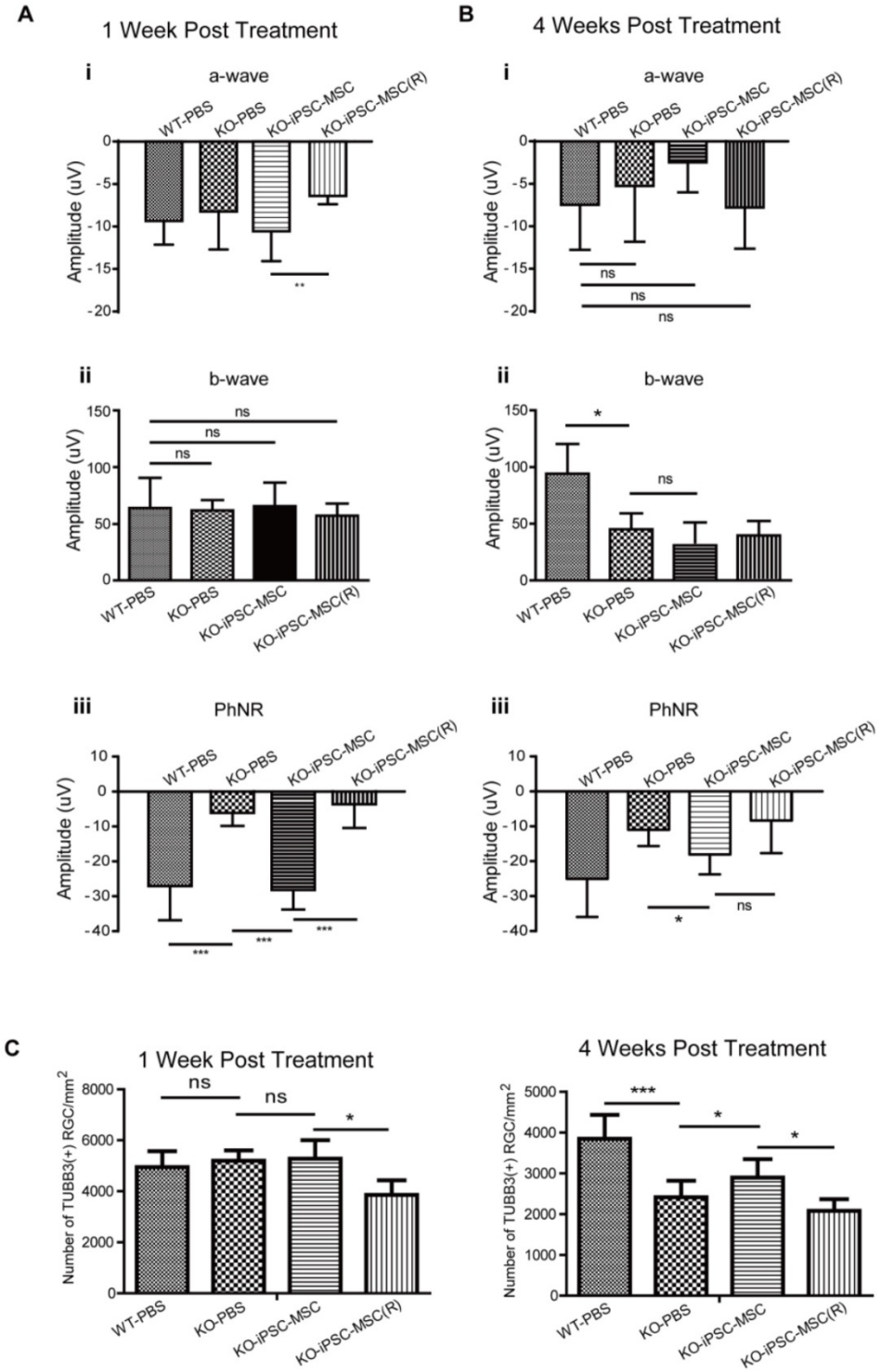

Figure 2. iPSC-MSCs administration prevented visual function decline and loss of retinal ganglion cell. A & B. After intravitreal administration, retinal function analysis by electroretinogram (ERG). (A) 1 week and (B) 4 weeks post injection, (i) a-wave, (ii) b-wave and (iii) PhRN amplitudes was recorded. (n=10). **C.** Density of RGC in the RGC layer immune labeled with TUBB3 antibody in WT mice and KO mice treated with PBS, MSC and MSC(R) were compared both at one week (upper lane) and four weeks (lower lane) after intravitreal injection. (n=5). Data information: In (A-C), data are presented as mean ± SD. *p<0.5, **p<0.01, ***p<0.001, ns, not significant (One-way ANOVA,).

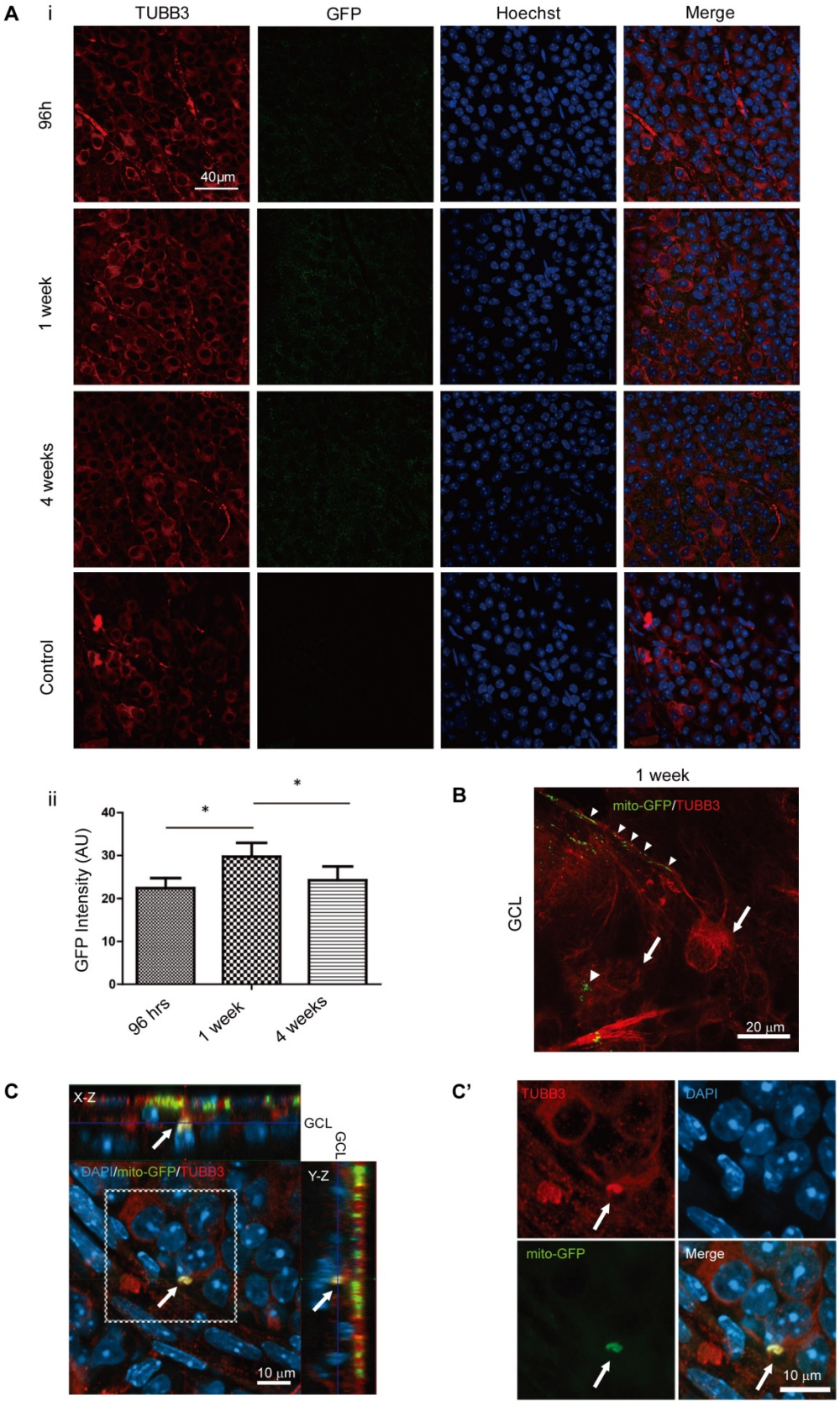

Figure 3. iPSC-MSCs transferred mitochondria to neurons in retinal ganglion cell layer. Ai. Representative images from GCL with immunostaining for anit-TUBB3 (red) and anti-GFP signals (green). Scale bar: 40 μm. Quantitative measurements fluorescence intensity of immune enhanced GFP in GCL (Aii). There was no fluorescence signal in PBS administration groups and the reading set as was as zero. Data are represented as mean fluorescence intensity ± SD (n=10, p-values calculated using One-way ANOVA, *p<0.05). **B.** 1 week post transplantation showed mito-GFP signals from mitochondria along the RGC axons (arrow heads) and cell body (arrows). Scale bars: 20 μm. **C.** iPSC-MSC transplanted *Ndufs4* KO mice retina was immunostained for TUBB3 (red). Effective transfer of LV-mito-GFP positive mitochondria overlapped with GCL retinal neurons (arrow; yellow). Cross section image shows the signal is localized to GCL. (C') higher magnification for dotted square in C. Scale bars: 10 μm.

To further prove those GFP enhanced signal was from transferred mitochondria, flat mounted retinas from 96 hours after intravitreal injection were investigated. Retinas were immunostained with anti-TUBB3 only and imaged in higher magnification with Z-stack scanning. The image clearly showed mito-GFP labeled mitochondria (Figure 3B; arrowheads) from iPSC-MSCs were trans-located within the RGC as outlined by TUBB3 (Figure 3B; arrows). This confirmed that GFP signal enhanced in Figure 3A i was from mito-GFP in the cells of GCL. Moreover, the orthogonal section showed mito-GFP positive mitochondria signals from iPSC-MSCs were detected within TUBB3 positive neuronal cell in the mouse GCL (Figure 3C, enlarged in 3C', arrows). This indicated that mitochondria in the cells of GCL were from iPSC-MSCs. Direct transfer of mitochondria from human iPSC-MSC to mouse RGCs was further confirmed in the co-culture system in vitro (Figure S2). These results suggested neuronal cells in the GCL directly received mitochondria from the injected human iPSC-MSCs to compensate mitochondrial deficiency in the KO mouse retinas.

Penetration of human iPSC-MSC mitochondria from iPSC-MSC but not iPSC-MSC itself into mouse retina

To determine whether injected iPSC-MSCs could penetrate the ILM and migrate into the mouse retina or just transfer healthy mitochondria of iPSC-MSCs into mouse retinal cells, mouse retinal samples were carefully examined for the presence of mice (M) and human (H) mitochondria (m) and nuclear (n) DNA traces using polymerase chain reaction (PCR) (Figure 4A) detection. Under dissection microscope, mouse retina was isolated from the underlying retinal pigmented epithelium and flatted with RGC face up. After removing vitreous body at the surface of ILM, it was quickly rinsed with saline before snap frozed for DNA extraction. Four pairs of primers designed for human specific nuclear DNA (H-nDNA), human specific mitochondrial DNA (H-mDNA), mice specific nuclear DNA (M-nDNA) and mice specific mitochondrial DNA (M-mDNA) were chosen [29]. PCR was performed on extracted mouse retinal DNA using specific primer pair at 96 hours, week 1 and 4 post injection. H-mDNA (Figure 4A ii, Lane 3), M-mDNA, and M-nDNA were detected in the retinal samples, but H-nDNA (Figure 4A ii, Lane 4) was not.

At 1 week post iPSC-MSC injection, at the vitreoretinal interface (VRI), human nuclear antigen (HNA) was detectable in VRI (Figure 4A iii upper panel) but not in GCL (Figure 4A iii lower panel). Immunostaining with human mitochondrial antibody (anti-hMito), hMito signal was co-localized with GFP signal of mitochondria (LV mito-GFP) from iPSC-MSCs in the VRI (Figure 4Bii; arrow). As expected, cells in the mouse retinal GCL positively stained with anti-Brn3a were surrounded by anti-hMito (Figure 4B iv; arrowheads) but not HNA (Figure 4A iii; lower panel). Importantly, many positive mitochondrial GFP signals (LV mito-GFP) were observed in TUBB3 positive GCL cells, (Figure 4B iii, arrowheads), further providing evidence that mitochondrial transfer but not iPSC-MSC migration occurs in the mouse retina.

VRI imaging was performed to determine the fate of transplanted cells post injection. Transplanted iPSC-MSCs with LV Mito-GFP formed a monolayer at the vitro retinal interface (VRI) at 96 hours and 1 week after injection (Figure 3C). VRI images showed mito-GFP signals and immunostaining of anti-hMito signals after 96 hours and 1 week post injection (Figure 4C, lower panel (X-Y)) and transferred mitochondria to the GCL (Figure 4C, upper panel (X-Z)). Surprisingly, the injected cells disappeared 4 weeks after injection and only donated human mitochondria detectable in the GCL (X-Z, anti-hMito, red). These results strongly suggest only mitochondria are transferred from transplanted cells and that donated mitochondria extend the longevity of RGC in the retina.

Müller cell activation and inflammatory response in whole retina of *Ndufs4* KO mice

To evaluate Müller cell activation following iPSC-MSC based therapy in complex I defect mice immunohistochemistry of GFAP was performed. GFAP is normally expressed in astrocytes of normal mouse retina. In response to retinal injury, GFAP gene transcription is strongly activated in the Müller cells and astrocytes. GFAP positive cells were limited in Müller cell end-feet and astrocytes in the nerve fiber layer and ganglion cell layer of the retina in WT control mice (Figure 5A). By week 7, the GFAP positive signal in KO mice had shown an axial extent throughout the retina with an increased intensity (Figure 5A-B). As shown in figure 5A-B, 4 weeks post iPSC-MSC treatment, reduced fluorescent intensity of GFAP staining had obviously declined in KO mice (KO+iPSC-MSC) retina compared with untreated KO mice (KO+PBS). These data indicate that iPSC-MSC could reduce abnormal activation of Müller cells in the mouse retina with defective mitochondria donation.

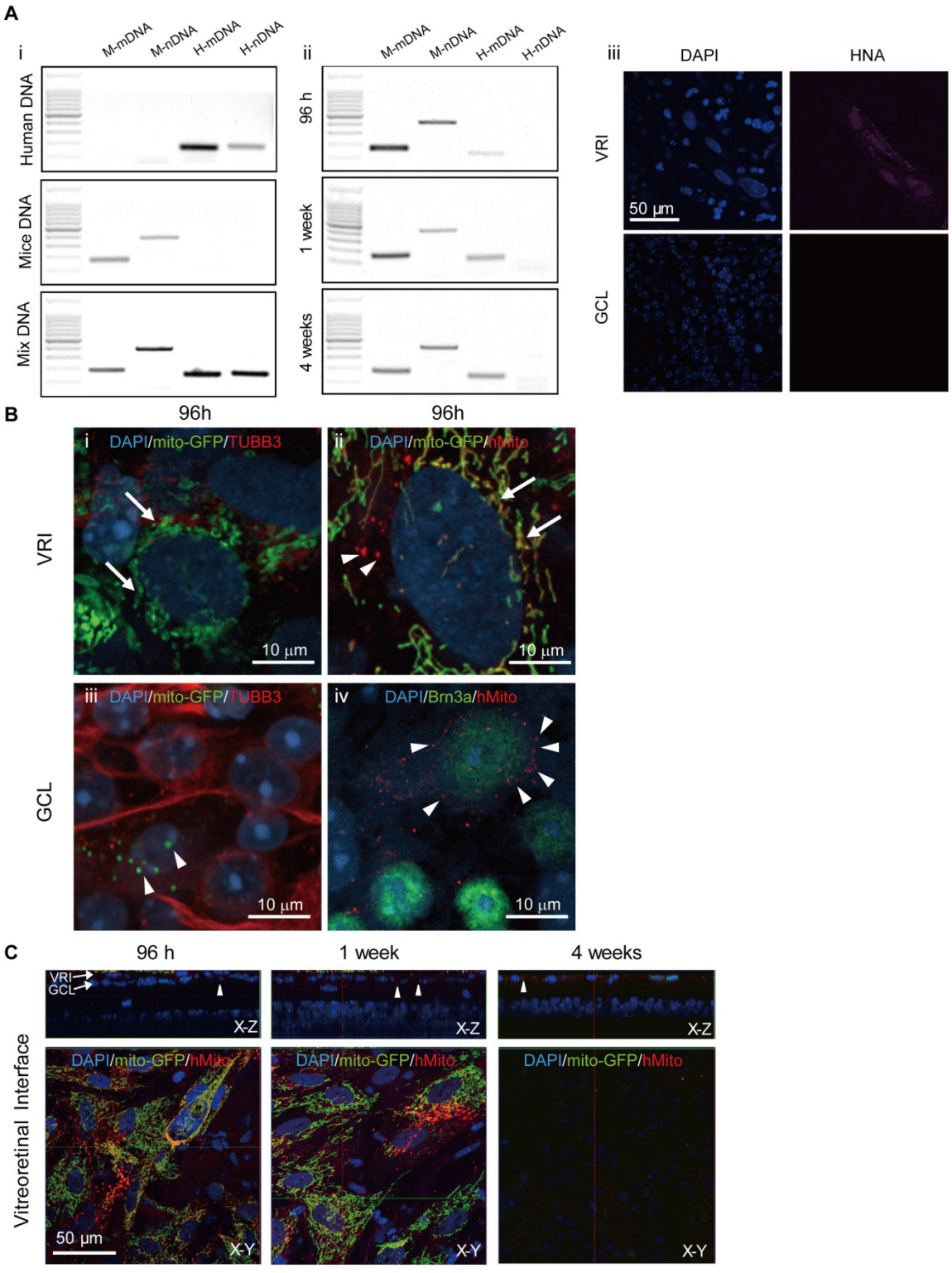

Figure 4. Detection of human mitochondrial within *Ndufs4* deficient mice. A. PCR results of retina tissue at 96 hours, 1 week and 4 weeks post treatment. DNA from human iPSC-MSCs, mice tissue and mixture (human cells + mice tissue) served as control to validate the primer amplification efficiency in panel (Ai). In all the time points, except H-nDNA, the other three including H-mDNA, M-nDNA, and M-mDNA could be detected in the mouse retinal samples (Aii). H-nDNA: human specific nuclear DNA, H-mDNA: human specific mitochondrial DNA, M-nDNA: mice specific nuclear DNA, M-mDNA: mice specific mitochondrial DNA. To confirm, HNA signal was detected in the VRI only but not GCL in the flat mounted mouse retinas at 1-week post injection (Aiii). Scale bar: 50 μm. **B.** At 96 hours post injection, positive mito-GFP but negative TUBB3 expression of iPSC-MSCs was detected in VRI (Green; arrows, Bi). These mito-GFP signals in VRI were overlapped with anti-hMito immunostained mitochondria (Red; arrows,Bii). Arrow head indicates human mitochondria labelled with anti-hMito but without mito-GFP in iPSC-MSC (Bii). In GCL the transferred mitochondria expressingmito-GFP signals (arrow heads) in the TUBB3 positive cells (Biii). Anti-hMito signals were detected in the cytoplasm of the Brn3a positive RGC cells (Red; arrow heads; Biv). Scale bars: 10 μm. **C.** Z-stack images showed iPSC-MSCs on VRI at different time post injection. iPSC-MSC cells expressing LV-Mito-GFP signals and immunostained anti-human mitochondria (anti-hMito, red) signals were detected at 96 hours and 1 week post injection but not 4 weeks. Anti-hMito signals existed in GCL surrounding RGCs were detected up to 4 weeks in the X-Z panel; arrow heads. DAPI (Blue). HNA - human nuclear antigen; VRI - vitreoretinal interface. Scale bars: 50 μm.

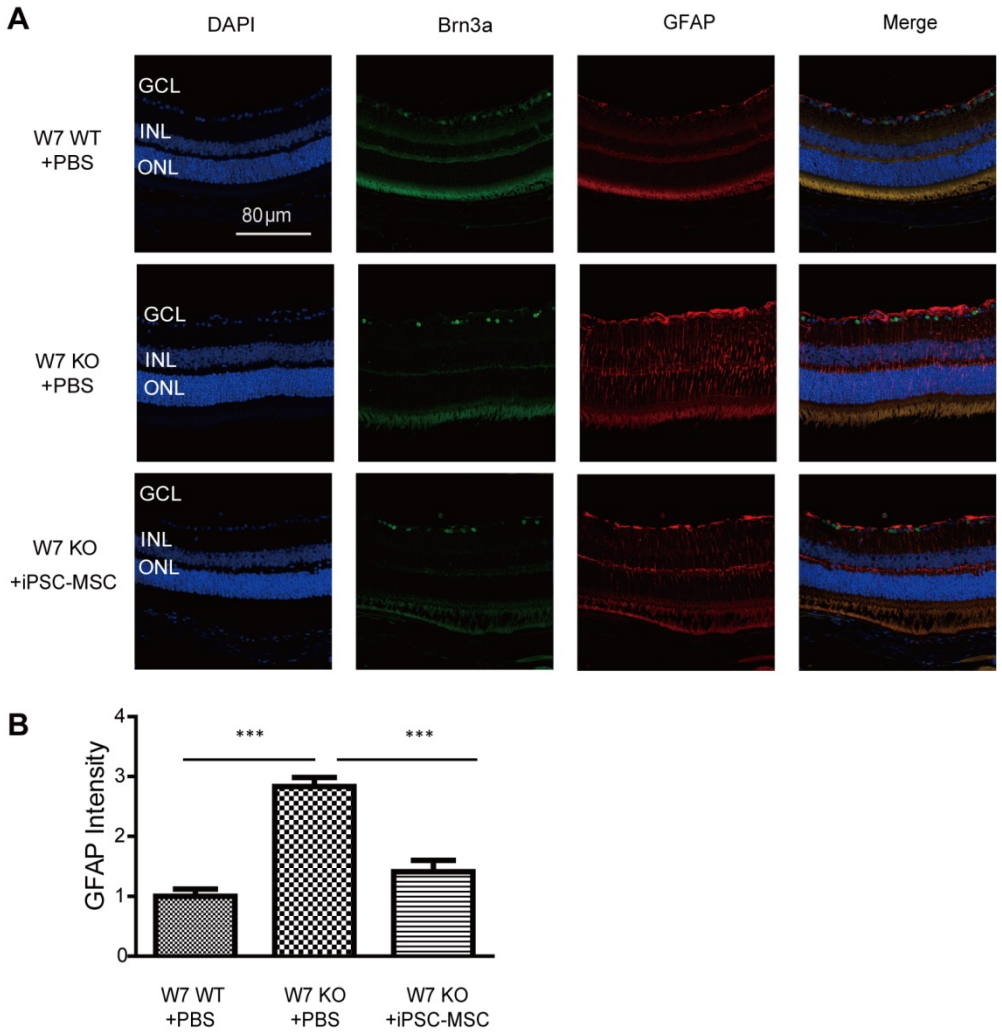

Figure 5. Astrocyte/Müller cell activation under iPSC-MSC transplantation. A. Retinal sections from WT, KO-PBS-injected, and KO-MSC-injected eyes were stained with Brn3a (green) and GFAP (red) antibodies. Sections were counterstained with DAPI (blue). GFAP staining was observed in GCL, INL and ONL retinas of 7 weeks of KO-PBS group while the retinas from KO-MSC treated group and WT showed less. The Scale bars: 80 μm. (GCL: ganglion cell layer; INL: inner nuclear layer; ONL: outer nuclear layer). **B.** GFAP intensity was analyzed from GCL to ONL layers. Compare to the KO-PBS group, the GFAP intensity was significantly suppressed in KO-MSC treated group (n=10, Error bar represent SD, ***p<0.001).

Mitochondrial complex I dysfunction in the retina is strongly related to an innate immune and inflammatory response [33]. Results of cytokine array and hierarchical clustering analysis of differential protein expression unveiled that *Ndufs4* KO mice (1 week KO+PBS/WT+PBS) are biased to an inflammatory status as evidenced by remarkably increased pro-inflammatory cytokines (i.e. CD30L, IL-5, TNFα, IFNγ etc.) but decreased anti-inflammatory cytokines and cell survival factors (i.e. IL-10, ICAM1etc.) (Figure 6, Figure S3). Notably, many of these prominently increased cytokines such as IL-17, IL-1β, TNFα, and CD30L [37-42] are associated with activation of NF-κB signaling pathway, a master signaling pathway in the regulation of inflammation. Importantly, 1 week post iPSC-MSC treatment, the enhanced pro-inflammatory cytokines had remarkably declined in the retina of KO mice compared to KO-PBS (1 week, KO+iPSC-MSC/KO+PBS), supporting effective protection of iPSC-MSC treatment in reduction of excessive inflammation. Nonetheless rotenone-treated iPSC-MSC(R) (1 week, KO+iPSC-MSC(R)/KO+PBS) lost protective ability when compared with the iPSC-MSC (1 week, KO+iPSC-MSC/KO+PBS). Of note, reduced pro-inflammatory cytokines (i.e. IL-17, IL-1β, IFNγ and CD30L etc.) after iPSC-MSC treatment (4 weeks, KO+iPSC-MSC/KO+PBS), but not iPSC-MSC(R) (4 weeks, KO+iPSC-MSC(R)/KO+PBS) were still evidenced up to 4 week post treatment (Figure 6, Figure S3). It indicates that increased inflammation in KO mice cannot be suppressed by iPSC-MSC(R) treatment but can be relieved by iPSC-MSC treatment after a single injection. This result illustrates distinct inflammatory status of WT and KO mice, and different therapeutic efficacy of iPSC-MSC and iPSC-MSC(R).

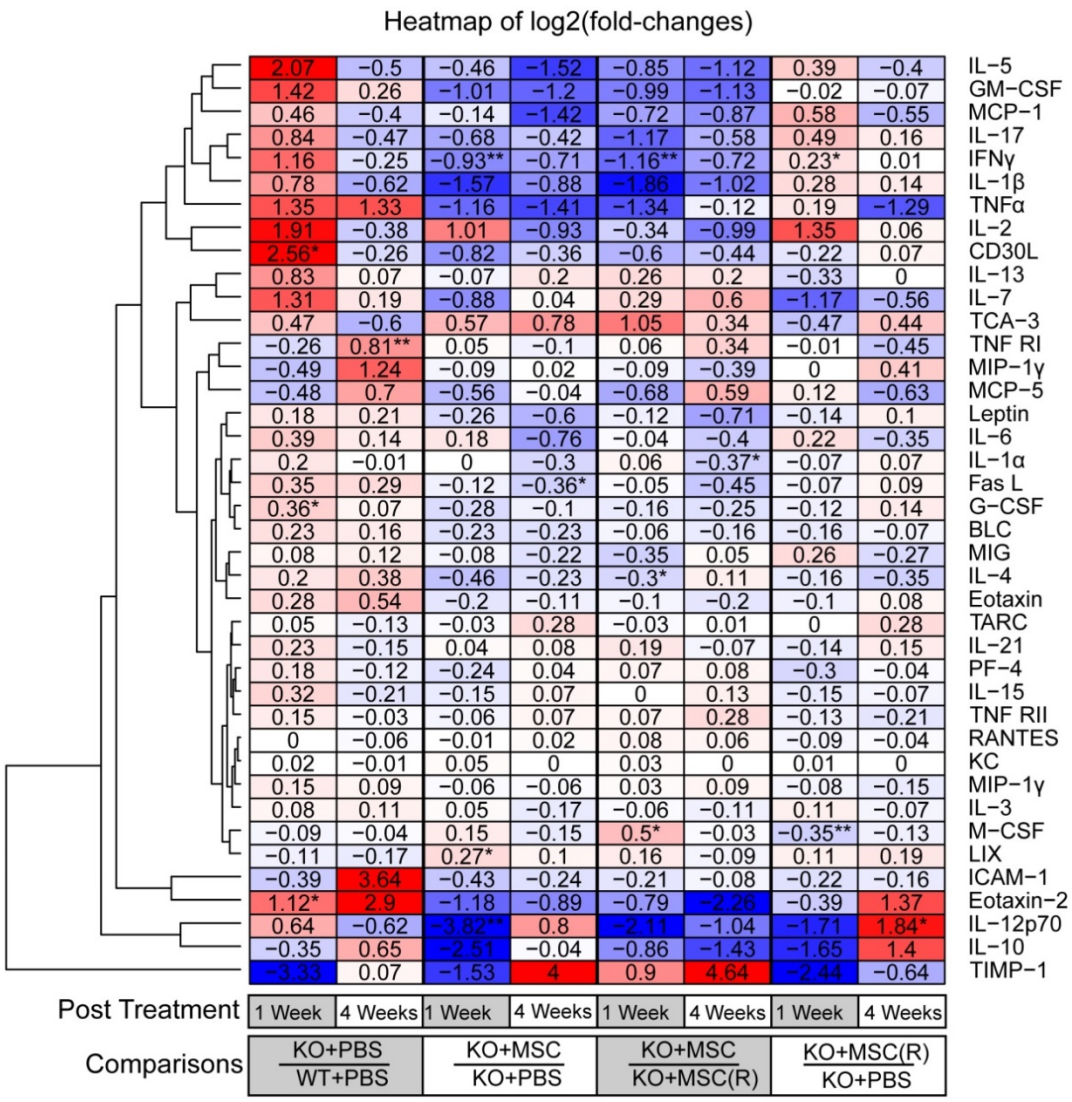

Figure 6. Fold-changes (log2) of cytokine concentrations in whole retina of Ndufs4 Mice. A heatmap showing the fold-changes (log2) of cytokine concentrations in whole retina under different conditions. One row represents one cytokine, one column represents one comparison. The value of each entry indicates a log2 (fold-change) of two concentrations, which is also represented by blue-red color-codes (blue: downregulated; white, no change; red: upregulated). The rows were ordered according to a hierarchical clustering of the fold-change values, by Euclidean distance. Four groups in experiments were compared at two time-points (1 week and 4 weeks post treatment respectively). (Student's t-test, *p<0.05, **p<0.01, ***p<0.05)

Discussion

In this study, we have demonstrated that RGCs display progressive functional defects and cell death in a *Ndufs4* knockout mouse model; iPSC-MSC delivered by intravitreal injection successfully delayed loss of RGC, preserved retinal function by donating mitochondria across the ILM to RGC; and help to suppress the abnormal activation of Müller cells and inflammatory status of the degenerating retina in *Ndufs4* KO mice.

iPSC-MSCs transferred their healthy mitochondria to the retina with a hereditary mitochondrial disorder via intravitreal injection. The mitochondrial transfer was detected 96 hours, 1 week and 4 weeks following injection. It is hard to precisely calculate the percentage of mitochondria transfer in RGC in vivo given the limitation on unequal transfer of human mitochondria in our experimental model. The vitreous chamber has been shown to be a favorable microenvironment for iPSC-MSC survival; iPSC-MSC remained in the vitreous cavity and had not integrated into the retina 1 week post treatment. Nevertheless, PCR results confirmed that only mitochondria of iPSC-MSCs could be transferred into the retina of mice after administration and none nuclei DNA of iPSC-MSC detected in the retina of *Ndufs4* mice. Those results are consistent with the data of Johnson et al. [43] who observed extremely poor retinal integration of MSCs following intravitreal injection. In some studies, the authors showed that injected cells remained in the vitreous cavity and did not integrate into the retina 12 weeks after treatment [44]. Due to the limited lifecycle of this mouse model

(around 9 weeks), we could not evaluate the maximal time for mitochondria transfer from iPSC-MSCs maintained within mice retina.

The mechanisms by which iPSC-MSCs support retinal regeneration are thought to be mainly via paracrine effects [13]. Our study proved that when iPSC-MSCs were pretreated with complex I inhibitor (Rot), the protective effect was diminished and the loss of RGC was increased comparable to the vehicle control group. In our previous study we had examined cytokines secreted by iPSC-MSCs and Rot-treated MSCs. It indicates that the secretion of interleukin-6 (IL-6), interleukin-8 (IL-8), vascular endothelial growth factor (VEGF) and monocyte chemotactic protein-1 (MCP-1) was no significant difference between iPSC-MSCs and Rot-treated MSCs [31]. It suggests that the functional protection afforded to RGC by mitochondrial transfer is independent to those paracrine effects. It further indicates that only healthy mitochondrion donated from iPSC-MSCs protect RGC against hereditary mitochondrial deficiency. Hence, mitochondrial transfer, as an important therapeutic mechanism, plays a vital role in such treatment. It is, therefore, intriguing to study the enhanced energy metabolism by mitochondrial donation for therapeutic interventions in retinal diseases. For instance, activation of AMPK by metformin to regulate metabolic homeostasis has been shown to promote survival of photoreceptors [45]. Increasing glucose uptake for aerobic glycolysis and increasing ATP levels by protein or gene delivery attenuated the loss of cones in rd1 animal [46]. These studies show that enhancing ATP production, mitochondrial DNA copy number, can rescue retinal cell loss in neurodegeneration. Our study demonstrated that iPSC-MSCs could directly transfer functionally healthy mitochondria in the mice retina to reduce retinal degeneration via regulation of retinal energy metabolism. However, the metabolic changes in the retinal neurons after mitochondria transfer require further investigations.

ERG assay was employed to evaluate retinal electrical responses [44]. Our results demonstrated that, at both 1- and 4-weeks post injection, the PhNR derives from retinal ganglion cells was preserved when treated with iPSC-MSCs. In addition, at 1 week after treatment, the amplitude of PhNR was increased in KO mice, when the RGC survival data remained unchanged. These results indicate that single injection of iPSC-MSC increased neuroprotective effect as early as 1-week post transplantation with reduced RGC loss.

Mitochondrial complex I dysfunction in the retina is strongly related to an innate immune and inflammatory response that results in loss of retinal ganglion cell function and death, as in Leber's hereditary Optic Neuropathy [33]. 4 weeks following iPSC-MSC treatment, glial fibrillary acidic protein (GFAP) expression was substantially reduced in the KO mice retinas. These results indicated that iPSC-MSCs could reduce abnormal activation of glial cells in the mouse retina with defective mitochondria. High levels of GFAP have been associated with pathological inflammation and RGC loss [47]. Secondary degeneration caused by the loss of primary retinal neuron degeneration significantly shorten the effective treatment window [18-20]. These features determine the crucial of the earlier intervention in RGC degeneration for the whole retinal health. Alfred et al., reported the activation of innate immunity, microglia and astrocyte released inflammatory cytokines and chemokine factors occurred even before retinal function deficits and reasonable cell loss in *Ndufs4* KO mice [33]. Cytokines protein-array revealed that proinflammatory cytokines were clearly increased in the retina of KO mice at week 4 compared with WT. It has been suggested that activation of microglia with IFN-g, GM-CSF and MCP-1 leads to neuronal injury [48-50]. In turn, activated microglia produced excessive IL-1 β and TNF α that are toxic to neurons [51, 52]. These results demonstrate a link between mitochondrial dysfunction (*Ndufs4* mutation) and inflammation that contributes to neural degeneration. Therefore, implications on management of the inflammatory response impose challenges for RGC survival in complex I dysfunction.

iPSC-MSC treatment in *Ndufs4*-KO mice effectively reduced neuroinflammatory cytokines such as TNF α, MIP−1g, GM-CSF, IL-5, IL-17 and IL-1 β [53, 54]. It is an obligatory role of NF-κB signaling in the regulation of mitochondrial transfer via TNT formation [55]. Interestingly, pro-inflammatory cytokines that were increased in *Ndufs4*-KO mice were down-regulated by iPSC-MSC treatment, such as GM-CSF, MCP-1, IL-17, IL-1 β TNF-α, IL−12p70 and CD30L, which were related to NF-κB pathway [37-42]. High production of cytokines such as TNF α and activation of NF-κB signaling in KO mice might be the trigger for mitochondrial transfer. We found that rotenone pretreated iPSC-MSC lost their protective effect, indicating that only the transferred healthy mitochondria produce beneficial effects to the affected retinas in addition to the paracrine effects. This is consistent with previous study that paracrine action and mitochondrial transfer is an interaction of two independent processes in MSC-mediated cell protection [56].

In previous study, we found iPSC-MSCs have advantages in mitochondrial transfer and therapeutic potentials to rescue cigarette smoke-induced lung damage and ovalbumin-induced asthma when compared with BM-MSC [6, 7]. In addition, we observed that mitochondrial morphology in the iPSC-MSC is different from those transferred mitochondria in RGC. The transferred mitochondria are normally smaller in recipient cells than that in donor iPSC-MSC. The size of mitochondria is determined by the balance between fission and fusion. Mitochondrial morphologies can change dramatically by shifting this balance. In some cells such as MSC they fuse together, forming a single closed network, whereas in other cells or under different circumstances mitochondrion convert into large numbers of small fragments. How the dynamics of mitochondrial morphology affects mitochondrial donation ability of iPSC-MSC deserve further study in the future.

Application of stem cell mitochondrial transfer opens new possibilities in the treatment for mitochondrial dysfunction related retinal diseases. Our finding provides the therapeutic potential of MSC for hereditary or acquired mitochondrial defects-provoked retinal degeneration (e.g. age related macular degeneration, glaucoma, diabetic retinopathy) [60-62]. MSC-modulated mitochondrial transfer may also enhance mitochondrial ability to resist retinal damages such as cold tolerance [63].

Conclusions

Mitochondrial defects caused by complex I deficiency induce retinal inflammation, visual dysfunction and retinal neuronal cell death. Intravitreal injection of human iPSC-MSCs can effectively donate functional mitochondria to mouse RGCs by overcoming the ILM barrier in the mouse retina. The donated mitochondria from iPSC-MSCs could restore RGC function against mitochondrial damage-induced excessive inflammation and retinal degeneration. These findings suggest that intravitreal iPSC-MSCs transplantation donated functional mitochondria to the inner retina (RGCs) and thus opens new possibilities to prevent or delay RGC degenerative responsive toacquired or hereditary mitochondrial disorders of the retina.

Abbreviations

Brn3a: Brain-specific homeobox/POU domain protein 3A; COX8: Cytochrome c oxidase subunit VIII; C-R: Central retina; DAPI: 4',6-diamidino-2-phenylindole; ERG: Electroretinography; F-P: Far-peripheral; GCL: Ganglion cell layer; GFP: Green fluorescent protein; H&E: Hematoxylin and eosin; INL: Inner Nuclear Layer; IPL: Inner plexiform layer; iPSCs: Induced pluripotent stem cells; KO: Knockout; LV: Lentiviral; M-P: Mid-peripheral; MSC: Mesenchymal stem cell; mtDNA: Mitochondrial DNA; nDNA: Nuclear DNA; N-P: Near peripheral; ONL: Outer nuclear layer; PCR: Polymerase chain reaction; RGC: Retina ganglion cell; Rot or R: Rotenone; TNF-α: Tumor necrosis factor α; TNTs: Tunneling nanotubes; TUBB3: Tubulin beta 3; WT: Wild-type; BLC/CXCL13: B lymphocyte chemoattractant; CD30L/TNFSF8: Tumor necrosis factor ligand superfamily 8; Eotaxin-1/CCL11: C-C motif chemokine 11; Eotaxin-2/MPIF-2/CCL24: Recombinant Human Eotaxin-2; Fas Ligand/TNFSF6: Fas Ligand Apo-1 Ligand, APT1 Ligand; GCSF: Granulocyte colony-stimulating factor; GM-CSF: Granulocyte-macrophage colony stimulating factor; I-309/TCA-3/CCL1: C-C motif chemokine 1; ICAM-1/CD54: Intercellular cell adhesion molecule-1; IFN-g: Recombinant Human Interferon-gamma; IL-1 alpha/IL-1 F1: Interleukin 1 alpha; IL-1β/IL-1 F2: Interleukin 1 beta; IL-10: Interleukin 10; IL-12 p70: Interleukin 12 p70; IL-13: Interleukin 13; IL-15: Interleukin 15; IL-17A: Interleukin-17A; IL-2: Interleukin 2; IL-21: Interleukin 21; IL-3: Interleukin 3; IL-4: Interleukin 4; IL-5: Interleukin 5; IL-6: Interleukin 6; IL-7: Interleukin 7; KC /CXCL1: chemokine (C-X-C motif) ligand 1; LIX/CXCL5: chemokine (C-X-C motif) ligand 5; MCP-1/CCL2: Monocyte chemoattractant protein-1; MCP-5: Monocyte chemoattractant protein-5; M-CSF: Macrophage colony-stimulating factor; MIG (CXCL9): Chemokine (C-X-C motif) ligand 9; MIP-1 alpha/CCL3: CC chemokine ligand 3; MIP-1 gamma: Macrophage inflammatory protein-1 gamma; Platelet Factor 4 (CXCL4) : Chemokine (C-X-C motif) ligand 4; RANTES/CCL5: CC chemokine ligand 5; TARC/CCL17: CC chemokine ligand 17; TIMP-1: Tissue inhibitor of metalloproteinases-1; TNF α: Tumor necrosis factor α; TNF RI/TNFRSF1A: tumor necrosis factor receptor I; and TNF RII/TNFRSF1B: Tumor necrosis factor receptor II.

Supplementary Material

Supplementary figures.
http://www.thno.org/v09p2395s1.pdf

Acknowledgements

This research was in part supported by National Natural Science Grant of China (No 31571407, 31270967 to Q Lian); Hong Kong Research Grant Council General Research Fund HKU17113816, HKU772510M to Q Lian); and the key grant from the Science and Technology Foundation of Guangdong Province of China (2015B020225001); Wenzhou

Medical University postdoctoral fellowship to D Jiang.

Author Contributions

DJ, GX, KC: experiments, collection and/or assembly of data, data analysis and manuscript drafting; HF, ZZ, LC, CM: preparation of MSC and collection of data; CL, SH, TL, YZ: collection of data; BY, PC, HT data analysis; KG, QF: data analysis and manuscript writing; QZ L: concept and design, data analysis, manuscript writing, and final approval of the manuscript.

Competing Interests

The authors have declared that no competing interest exists.

References

1. Inoue Y, Iriyama A, Ueno S, Takahashi H, Kondo M, Tamaki Y, et al. Subretinal transplantation of bone marrow mesenchymal stem cells delays retinal degeneration in the RCS rat model of retinal degeneration. Exp Eye Res. 2007; 85: 234-41.
2. Johnson TV, Bull ND, Hunt DP, Marina N, Tomarev SI, Martin KR. Neuroprotective Effects of Intravitreal Mesenchymal Stem Cell Transplantation in Experimental Glaucoma. Invest Ophthalmol Vis Sci. 2010; 51: 2051-59.
3. Ng TK, Fortino VR, Pelaez D, Cheung HS. Progress of mesenchymal stem cell therapy for neural and retinal diseases. World J Stem Cells. 2014; 6: 111-9.
4. Yu-Wai-Man P, Votruba M, Moore AT, Chinnery PF. Treatment strategies for inherited optic neuropathies: past, present and future. Eye. 2014; 28: 521-37.
5. Kicic A, Shen WY, Wilson AS, Constable IJ, Robertson T, Rakoczy PE. Differentiation of marrow stromal cells into photoreceptors in the rat eye. J Neurosci. 2003; 23: 7742-9.
6. Phinney DG, Prockop DJ. Concise review: Mesenchymal stem/multipotent stromal cells: The state of transdifferentiation and modes of tissue repair - Current views. Stem cells. 2007; 25: 2896-902.
7. Joe AW, Gregory-Evans K. Mesenchymal Stem Cells and Potential Applications in Treating Ocular Disease. Curr Eye Res. 2010; 35: 941-52.
8. Tomita M, Mori T, Maruyama K, Zahir T, Ward M, Umezawa A, et al. A comparison of neural differentiation and retinal transplantation with bone marrow-derived cells and retinal progenitor cells. Stem cells. 2006; 24: 2270-8.
9. Ratajczak MZ, Kucia M, Reca R, Majka M, Janowska-Wieczorek A, Ratajczak J. Stem cell plasticity revisited: CXCR4-positive cells expressing mRNA for early muscle, liver and neural cells 'hide out' in the bone marrow. Leukemia. 2004; 18: 29-40.
10. Gnecchi M, He H, Liang OD, Melo LG, Morello F, Mu H, et al. Paracrine action accounts for marked protection of ischemic heart by Akt-modified mesenchymal stem cells. Nat Med. 2005;11:367-8
11. Manuguerra-Gagne R, Boulos PR, Ammar A, Leblond FA, Krosl G, Pichette V, et al. Transplantation of mesenchymal stem cells promotes tissue regeneration in a glaucoma model through laser-induced paracrine factor secretion and progenitor cell recruitment. Stem cells. 2013; 31: 1136-48.
12. Torrente Y, Polli E. Mesenchymal stem cell transplantation for neurodegenerative diseases. Cell Transplant. 2008; 17: 1103-13.
13. Cislo-Pakuluk A, Marycz K. A promising tool in retina regeneration: current perspectives and challenges when using mesenchymal progenitor stem cells in veterinary and human ophthalmological applications. Stem Cell Rev Rep. 2017; 13: 598-602.
14. London A, Benhar I, Schwartz M. The retina as a window to the brain-from eye research to CNS disorders. Nat Rev Neurol. 2013; 9: 44-53.
15. Rodieck RW. Quantitative analysis of cat retinal ganglion cell response to visual stimuli. Vision Res. 1965; 5: 583-601.
16. Almasieh M, Wilson AM, Morquette B, Cueva Vargas JL, Di Polo A. The molecular basis of retinal ganglion cell death in glaucoma. Prog Retin Eye Res. 2012; 31: 152-81.
17. Aguayo AJ, Bray GM, Rasminsky M, Zwimpfer T, Carter D, Vidal-Sanz M. Synaptic connections made by axons regenerating in the central nervous system of adult mammals. J Exp Biol. 1990; 153: 199-224.
18. Goldberg JL, Klassen MP, Hua Y, Barres BA. Amacrine-signaled loss of intrinsic axon growth ability by retinal ganglion cells. Science. 2002; 296: 1860-4.
19. Levkovitch-Verbin H, Quigley HA, Kerrigan-Baumrind LA, D'Anna SA, Kerrigan D, Pease ME. Optic nerve transection in monkeys may result in secondary degeneration of retinal ganglion cells. Invest Ophthalmol Vis Sci. 2001; 42: 975-82.
20. Hilla AM, Diekmann H, Fischer D. Microglia Are Irrelevant for Neuronal Degeneration and Axon Regeneration after Acute Injury. J Neurosci. 2017; 37: 6113-24.
21. Quigley HA, Iglesia DS. Stem cells to replace the optic nerve. Eye. 2004; 18: 1085-8.
22. Rustom A, Saffrich R, Markovic I, Walther P, Gerdes HH. Nanotubular highways for intercellular organelle transport. Science. 2004; 303: 1007-10.
23. Islam MN, Das SR, Emin MT, Wei M, Sun L, Westphalen K, et al. Mitochondrial transfer from bone-marrow-derived stromal cells to pulmonary alveoli protects against acute lung injury. Nat Med. 2012; 18: 759-65.
24. Plotnikov EY, Khryapenkova TG, Vasileva AK, Marey MV, Galkina SI, Isaev NK, et al. Cell-to-cell cross-talk between mesenchymal stem cells and cardiomyocytes in co-culture. J Cell Mol Med. 2008; 12: 1622-31.
25. Spees JL, Olson SD, Whitney MJ, Prockop DJ. Mitochondrial transfer between cells can rescue aerobic respiration. Proc Natl Acad Sci U S A. 2006; 103: 1283-8.
26. Jiang D, Gao F, Zhang Y, Wong DS, Li Q, Tse HF, et al. Mitochondrial transfer of mesenchymal stem cells effectively protects corneal epithelial cells from mitochondrial damage. Cell Death Dis. 2016; 7: e2467.
27. Boukelmoune N, Chiu GS, Kavelaars A, Heijnen CJ. Mitochondrial transfer from mesenchymal stem cells to neural stem cells protects against the neurotoxic effects of cisplatin. Acta Neuropathol Commun. 2018; 6: 139.
28. Babenko VA, Silachev DN, Popkov VA, Zorova LD, Pevzner IB, Plotnikov EY, et al. Miro1 enhances mitochondria transfer from multipotent mesenchymal stem cells (mmsc) to neural cells and improves the efficacy of cell recovery. Molecules. 2018; 23: 687.
29. Li X, Michaeloudes C, Zhang YL, Wiegman CH, Adcock IM, Lian QZ, et al. Mesenchymal stem cells alleviate oxidative stress-induced mitochondrial dysfunction in the airways. J Allergy Clin Immunol. 2018; 141(5):1634-45.
30. Yao Y, Fan XL, Jiang D, Zhang YL, Li X, Xu ZB, et al. Connexin 43-mediated mitochondrial transfer of ipsc-mscs alleviates asthma inflammation. Stem Cell Rep. 2018; 11: 1120-35.
31. Zhang Y, Yu Z, Jiang D, Liang X, Liao S, Zhang Z, et al. iPSC-MSCs with high intrinsic miro1 and sensitivity to tnf-alpha yield efficacious mitochondrial transfer to rescue anthracycline-induced cardiomyopathy. Stem Cell Rep. 2016; 7: 749-63.
32. Kruse SE, Watt WC, Marcinek DJ, Kapur RP, Schenkman KA, Palmiter RD. Mice with mitochondrial complex I deficiency develop a fatal encephalomyopathy. Cell Metab. 2008; 7(4): 312-20.
33. Yu AK, Song L, Murray KD, van der List D, Sun C, Shen Y, et al. Mitochondrial complex I deficiency leads to inflammation and retinal ganglion cell death in the Ndufs4 mouse. Hum Mol Genet. 2015; 24: 2848-60.
34. Lian Q, Zhang Y, Zhang J, Zhang HK, Wu X, Zhang Y, et al. Functional mesenchymal stem cells derived from human induced pluripotent stem cells attenuate limb ischemia in mice. Circulation. 2010; 121: 1113-23.
35. Dull T, Zufferey R, Kelly M, Mandel RJ, Nguyen M, Trono D, et al. A third-generation lentivirus vector with a conditional packaging system. J Virol. 1998; 72: 8463-71.
36. Sappington RM, Chan M, Calkins DJ. Interleukin-6 protects retinal ganglion cells from pressure-induced death. Invest Ophthalmol Vis Sci. 2006; 47: 2932-42.
37. Infante-Duarte C, Horton HF, Byrne MC, Kamradt T. Microbial lipopeptides induce the production of IL-17 in Th cells. J Immunol. 2000; 165: 6107-15.
38. Bonizzi G, Karin M. The two NF-kappa B activation pathways and their role in innate and adaptive immunity. Trends Immunol. 2004; 25: 280-8.
39. Jovanovic DV, Di Battista JA, Martel-Pelletier J, Jolicoeur FC, He Y, Zhang M, et al. IL-17 stimulates the production and expression of proinflammatory cytokines, IL-beta and TNF-alpha, by human macrophages. J Immunol. 1998; 160: 3513-21.
40. Abdalla SA, Horiuchi H, Furusawa S, Matsuda H. Molecular cloning and characterization of chicken tumor necrosis factor (TNF)-superfamily ligands, CD30L and TNF-related apoptosis inducing ligand (TRAIL). J Vet Med Sci. 2004; 66: 643-50.
41. Yue SC, Shaulov A, Wang RJ, Balk SP, Exley MA. CD1d ligation on human monocytes directly signals rapid NF-kappa B activation and production of bioactive IL-12. Proc Natl Acad Sci U S A. 2005; 102: 11811-6.
42. Franchi L, Amer A, Body-Malapel M, Kanneganti TD, Ozoren N, Jagirdar R, et al. Cytosolic flagellin requires Ipaf for activation of caspase-1 and interleukin 1 beta in salmonella-infected macrophages. Nat Immunol. 2006; 7: 576-82.
43. Johnson TV, Bull ND, Martin KR. Identification of barriers to retinal engraftment of transplanted stem cells. Invest Ophthalmol Vis Sci. 2010; 51: 960-70.
44. Ezquer M, Urzua CA, Montecino S, Leal K, Conget P, Ezquer F. Intravitreal administration of multipotent mesenchymal stromal cells triggers a cytoprotective microenvironment in the retina of diabetic mice. Stem Cell Res Ther. 2016; 7: 42.
45. Xu L, Kong L, Wang JG, Ash JD. Stimulation of AMPK prevents degeneration of photoreceptors and the retinal pigment epithelium. Proc Natl Acad Sci U S A. 2018; 115: 10475-80.
46. Ait-Ali N, Fridlich R, Millet-Puel G, Clerin E, Delalande F, Jaillard C, et al. Rod-Derived Cone Viability Factor Promotes Cone Survival by Stimulating Aerobic Glycolysis. Cell. 2015; 161: 817-32.

47. Kurihara T, Ozawa Y, Shinoda K, Nagai N, Inoue M, Oike Y, et al. Neuroprotective effects of angiotensin II type 1 receptor (AT1R) blocker, telmisartan, via modulating AT1R and AT2R signaling in retinal inflammation. Invest Ophthalmol Vis Sci. 2006; 47: 5545-52.
48. Lin HW, Levison SW. Context-dependent IL-6 potentiation of interferon-gamma-induced IL-12 secretion and CD40 expression in murine microglia. J Neurochem. 2009; 111: 808-18.
49. Vargas DL, Nascimbene C, Krishnan C, Zimmerman AW, Pardo CA. Neuroglial activation and neuroinflammation in the brain of patients with autism. Ann Neurol. 2005; 57: 67-81.
50. Meda L, Cassatella MA, Szendrei GI, Otvos L, Jr., Baron P, Villalba M, et al. Activation of microglial cells by beta-amyloid protein and interferon-gamma. Nature. 1995; 374: 647-50.
51. Block ML, Hong JS. Microglia and inflammation-mediated neurodegeneration: multiple triggers with a common mechanism. Prog Neurobiol. 2005; 76: 77-98.
52. Chi W, Li F, Chen H, Wang Y, Zhu Y, Yang X, et al. Caspase-8 promotes NLRP1/NLRP3 inflammasome activation and IL-1beta production in acute glaucoma. Proc Natl Acad Sci U S A. 2014; 111: 11181-6.
53. Yuan L, Neufeld AH. Tumor necrosis factor-alpha: a potentially neurodestructive cytokine produced by glia in the human glaucomatous optic nerve head. Glia. 2000; 32: 42-50.
54. Murray PJ, Wynn TA. Protective and pathogenic functions of macrophage subsets. Nat Rev Immunol. 2011; 11: 723-37.
55. Ahmad T, Mukherjee S, Pattnaik B, Kumar M, Singh S, Kumar M, et al. Miro1 regulates intercellular mitochondrial transport & enhances mesenchymal stem cell rescue efficacy. EMBO J. 2014; 33: 994-1010.
56. Vallabhaneni KC, Haller H, Dumler I. Vascular smooth muscle cells initiate proliferation of mesenchymal stem cells by mitochondrial transfer via tunneling nanotubes. Stem Cells Dev. 2012; 21: 3104-13.
57. Alston CL, Rocha MC, Lax NZ, Turnbull DM, Taylor RW. The genetics and pathology of mitochondrial disease. J Pathol. 2017; 241: 236-50.
58. Liesa M, Palacin M, Zorzano A. Mitochondrial dynamics in mammalian health and disease. Physiol Rev 2009; 89: 799-845.
59. Deng WL, Gao ML, Lei XL, Lv JN, Zhao H, He KW, et al. Gene correction reverses ciliopathy and photoreceptor loss in ipsc-derived retinal organoids from retinitis pigmentosa patients. Stem cell Rep. 2018; 10: 1267-81.
60. Ding X, Patel M, Chan CC. Molecular pathology of age-related macular degeneration. Prog Retin Eye Res. 2009; 28: 1-18.
61. Chrysostomou V, Rezania F, Trounce IA, Crowston JG. Oxidative stress and mitochondrial dysfunction in glaucoma. Curr Opin Pharmacol. 2013; 13: 12-15.
62. Giacco F, Brownlee M. Oxidative stress and diabetic complications. Circ Res. 2010; 107: 1058.
63. Ou J, Ball JM, Luan Y, Zhao T, Miyagishima KJ, Xu Y, et al. iPSCs from a Hibernator Provide a Platform for Studying Cold Adaptation and Its Potential Medical Applications. Cell. 2018; 173: 851-63.